Fast Differential Phase-Contrast Imaging and Total Fluorescence Yield Mapping in a Hard X-ray Fluorescence Microprobe

S. Vogt*, M. Feser+, D. Legnini*, J. Kirz+, J. Maser*

* *Advanced Photon Source, Argonne National Laboratory, 9700 S. Cass Av., Argonne, IL 60439, U. S. A.*
+ *Department of Physics and Astronomy, State University of New York at Stony Brook, Stony Brook, NY 11794, U. S. A.*

Abstract. We have incorporated differential phase-contrast (DPC) detection in a hard x-ray fluorescence microprobe at the Advanced Photon Source. We report a straightforward implementation of unidirectional DPC and demonstrate that it is highly advantageous for imaging low-Z specimens with hard x-rays (10keV). Phase-contrast imaging of a specimen can be used to acquire fast overview images of samples that allow more precise targeting of time consuming fluorescence scans. In order to get an overview of the elemental content of a specimen in these fly-scans, we have also implemented a fast detection of total fluorescence yield. Additionally, a DPC image of the specimen is obtained simultaneously with the fluorescence maps in normal step-scanning mode, to facilitate a direct comparison and co-registration with visible light micrographs.

INTRODUCTION

The roles of trace metals in the biological and medical sciences is a scientific question whose importance has received increased recognition (see, e.g., [1]). Synchrotron based x-ray fluorescence (XRF) microscopy is a powerful technique to study the extra- and intracellular distributions of the elements from Si to Zn and above. Due to its low background, XRF is particularly well suited to detect elements in trace quantities, down to the level of attograms. Typically, hard x-rays (e.g., E=10 keV) are focused with high-resolution x-ray optics (e.g., zone plates) onto the sample which is raster scanned through the focal spot. At each specimen position, a XRF spectrum is acquired using an energy-dispersive x-ray detector, from which the trace metal quantities can then be determined.

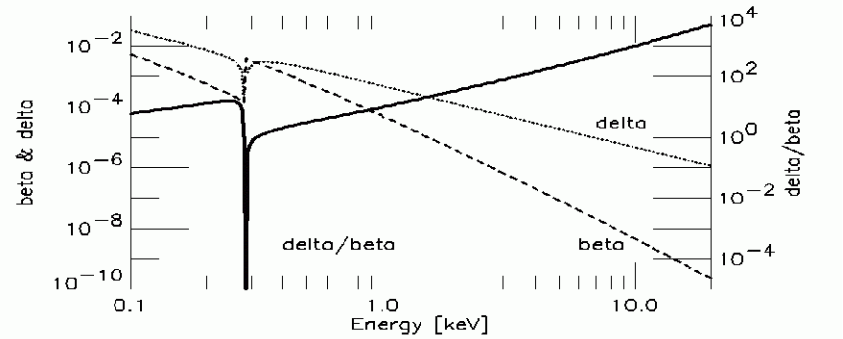

FIGURE 1. Plot of the components δ and β of the complex index of refraction n=1-δ-iβ of carbon. The real part, δ, is related to the phase shift in the specimen, the imaginary part, β, to photoelectric absorption. This graph shows the increasing significance of the phase part δ with higher x-ray energy. For example, the ratio δ/β, which is indicative of the relative strength of phase and absorption contrast, is about 2 orders of magnitude higher at E=10 keV than it is at 1 keV.

CP705, *Synchrotron Radiation Instrumentation: Eighth International Conference,* edited by T. Warwick et al.

Most of the mass of a (dried) biological cell, however, typically is made up of C, N, and O, elements which are difficult to map using XRF due to their small absorption cross-section and low fluorescence yield. The small photo-electric absorption cross-section of carbon and other low-Z elements also make the direct visualization of cells in absorption contrast at high x-ray energies difficult. However, at high x-ray energies the real part δ of the complex index of refraction $n=1-\delta-i\beta$ is several orders of magnitude larger than the imaginary part β (see, e.g., Fig. 1). This can be used advantageously to visualize biological material in phase instead of absorption contrast [2,3,4].

METHOD & INSTRUMENTATION

Different kinds of phase based contrast can be visualized in a scanning microscope type setup. In Nomarski differential interference (DIC) setup, for example, two zone plates are aligned in optical near field such that two virtual x-ray sources are created, whose interaction with the sample cause object dependent interference fringes in the detector plane. With spatially resolving detector a DIC image can then be built up [5]. However, the creation of two virtual sources leads to two slightly displaced focal spots causing a small loss of spatial resolution.

Differential phase contrast (DPC) makes direct use of x-rays that were refracted by the specimen, therefore it does not require changes to focusing optics, and in particular, it does not need two x-ray sources. The macroscopic description of DPC is governed by the spatially varying real part of the complex index of refraction n. While the total transmitted flux is insensitive to these phase effects, they lead to spatial variations in the far field diffraction pattern, which can be registered with appropriate detectors. A schematic illustration is shown in Fig. 2.

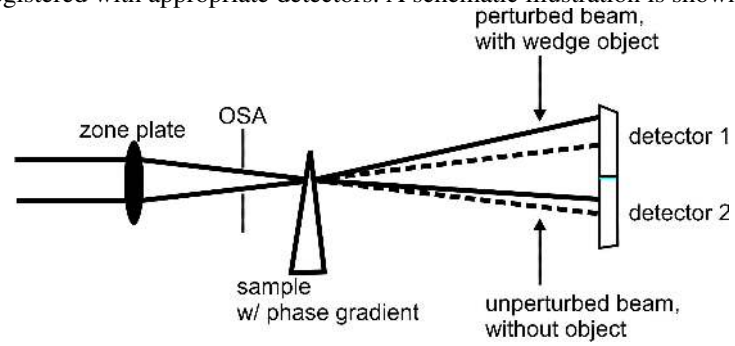

FIGURE 2. Illustration of differential phase contrast in a scanning microprobe setup. The zone plate focuses hard x-rays into a focal spot on the sample. The order sorting aperture (OSA) suppresses any x-rays not diffracted into the first (focusing) order. Here, the presence of a wedge shaped phase object causes an angular shift of the center of the transmitted beam. By using a set of spatially resolving detectors this shift can be measured. Note that, in contrast to visible light, x-rays are deflected away from the thicker phase material. This effect is due to the real part of the complex refraction ($n_{real} = 1-\delta$) being slightly smaller than 1, in contrast to typical indices of refraction for visible light which are larger than one.

The use of quadrant detectors to visualize phase information has been studied for electron microscopy [6] and been applied to soft x-ray microscopy [7,8,9]. To investigate the feasibility of differential phase contrast at ~10 keV, we have performed experiments at the sector 2 side-branch hard x-ray microprobe at the Advanced Photon Source (2-ID-E). We have chosen a very simple setup as shown in Fig. 3, where we were able to implement DPC with the addition of a motor driven razor blade and an additional ion chamber. x-rays are generated by an undulator with a periodicity of either 3.3 or 5.5 cm. A silicon <111> crystal intercepts part of the x-ray beam, and deflects it into the side branch station. An upstream pinhole is used to define the x-ray beam and block x-rays outside the aperture of the zone plate, in order to reduce the background as far upstream as possible. This component is followed by an ionchamber which is used to measure the incident flux, and as such is also employed for normalization of the transmitted x-ray signal. A stacked pair of Fresnel zone plates to maximize focused flux [10,11] in conjunction with an order sorting aperture (OSA) focuses the x-rays onto the sample. Next to the OSA a photodiode (SXUV-100, Intern. Radiation Detectors, Inc., 100 mm^2 sensitive area) is mounted to allow the fast collection of x-rays originating from the sample over a large solid angle. This signal is a total fluorescence yield (TFY) map, integrating over all the x-ray fluorescence plus a contribution from elastic and inelastic scattering processes. It is a good measure for the total medium to heavy elemental content.

An ionchamber downstream of the sample (DS IC) measures the transmitted x-ray flux. A razor blade behind the DS IC is moved partly into the beam so as to block the lower half plane of the unperturbed transmitted x-ray beam, which effectively makes the third ion chamber (DPC IC) only sensitive to the upper half plane. For fully coherent

illumination, the image recorded on this detector is in good approximation the vertical derivative of the phase transmission function of the specimen [6] and hence gives a unidirectional differential phase contrast image of the specimen. To remove the influence of beam intensity variations, the signal of the half plane detector is normalized by the total transmitted flux signal.

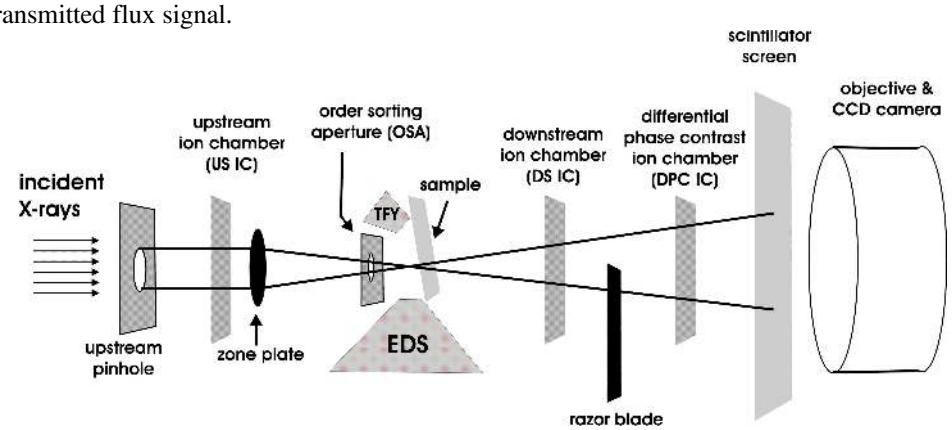

FIGURE 3. Illustration of the setup at the 2-ID-E beamline at the Advanced Photon Source. A razor blade is introduced between DS and DPC ICs, so that the 50% of the unperturbed transmitted beam is blocked. Differential phase contrast is then calculated by comparison of DPC IC with DS IC. A 10x10mm^2 photodiode is used to detect the total fluorescence yield (TFY), in particular for fast scans. An energy dispersive LeGe detector (EDS) resolves the energy of XRF photons for slow step scans. A scintillator screen with a microscope objective and a CCD camera allows a direct view of the projected x-rays; it is only used for coarse alignment of the specimen.

RESULTS

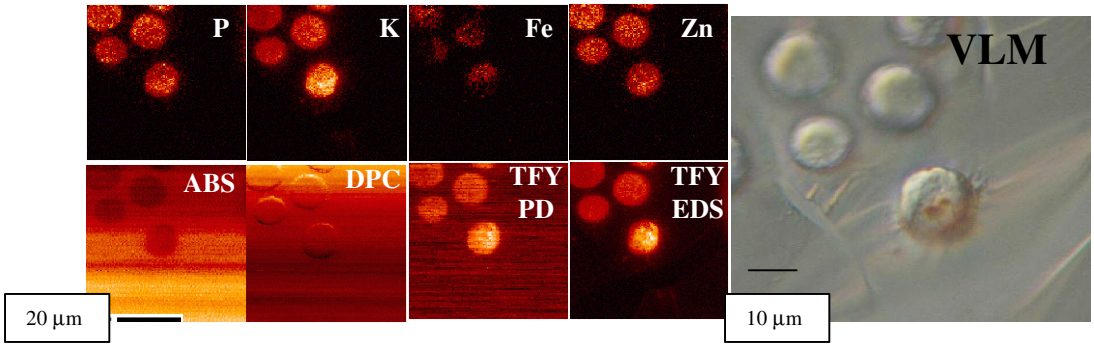

FIGURE 4. P - Zn: selected elemental maps generated from detected x-ray fluorescence spectra of a step scan of a group of HL60 cells (50x50 microns, 1 second dwell time, 10 keV incident Energy), **ABS**: absorption contrast image resulting from division of DS IC by US IC. **DPC**: unidirectional differential phase contrast, calculated by division of DPC IC by DS IC. **TFY-EDS:** total fluorescence yield as measured by the energy dispersive x-ray detector. **TFY-PD**: total fluorescence yield as measured by a photodiode mounted near the OSA. **VLM**: visible light micrograph of the HL60 cell group.

We tested the above scheme in two different operation modes. In step scan mode, the mode for slow scanning a specimen during acquisition of x-ray fluorescence spectra, we were able to acquire differential phase images simultaneous to the acquisition of x-ray fluorescence maps. Fig. 4 shows selected images from such a scan of a group of HL-60 cells, as well as a visible light micrograph of the same area. In DPC contrast, the cells can be clearly identified. The unidirectionality of the setup becomes evident in the fact that DPC is only visible in the vertical direction, as this was the direction selected by the knife edge. In horizontal direction, parallel to the knife edge, no DPC contrast is visible.

In fly scan mode, the goal is to quickly scan a sample area without using the time consuming energy dispersive x-ray detector, while still being able to identify cells and differentiate between cells and dust particles, debris and other organic remnants. This allows one to exactly locate specific sample areas of interest for later high resolution step scans. For this purpose we employ both DPC and TFY contrast. Fig. 5 is an example that was taken of the same sample region as shown in Fig. 4. Even at 5 ms dwell times, the cells can be easily made out. The DPC helps to

confirm that the visualized objects are organic matter, and the TFY signal is used to ascertain that the objects do contain medium to high Z materials and are not just cell debris.

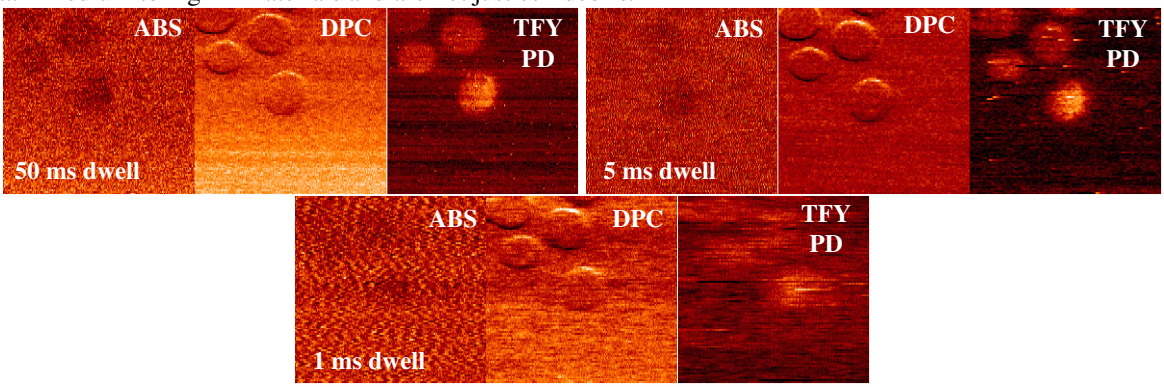

FIGURE 5. Fly scan images of a group of HL60 cells with different dwell times in absorption contrast, differential phase contrast and total fluorescence yield. Each scan size is 50x50 microns. While cell detection in absorption contrast is quickly limited by insufficient photon statistics, the detection of the DPC and TFY signals is limited in the current system by the speed of the amplifiers used to read the photodiode and ionchamber currents.

CONCLUSIONS AND OUTLOOK

We have shown that differential phase contrast provides excellent contrast for carbon based biological mass. It can be easily acquired simultaneously to the acquisition of spectral data, without the need for any compromises in the instrument. A simple setup with two ion chambers and a motorized razor blade is a very cost effective and efficient way to provide unidirectional DPC. The combination of DPC and photodiode based total fluorescence yield detection provides excellent signals for fast fly scans to find cells and sample regions quickly. Dwell times of 5 ms are well matched to our current detector systems, 1 ms are possible.

We are working on a dedicated configured detector system, adapted from soft x-ray microscopy [12,13]. Preliminary experiments have shown that such a setup should be able to deliver DPC in all directions, at truly photon statistics limited dwell times, thus enabling dwell times as low as 0.1 ms.

ACKNOWLEDGMENTS

The authors wish to thank D. Glesne, T. Paunesku, N. Stoijevic, and G. Woloschak for providing samples. Use of the Advanced Photon Source was supported by the U.S. Department of Energy, Basic Energy Sciences, under Contract No. W-31-109-ENG-38.

REFERENCES

1. Ash, C. and Stone, R., Science 300, 925 (2003)
2. Schmahl, G., Rudolph, D., Schneider, G., Guttmann, P., and Niemann, B., Optik 97, 181-182 (1994)
3. Kaulich, B., Polack, F., Neuhaeusler, U., Susini, J., di Fabrizio, E., and Wilhein, T., Optics Expr. 10:20, 1111-1117 (2002)
4. Kagoshima, Y., *et al.*, J. Phys IV France 104, 49-52 (2003)
5. Wilhein, T., *et al.*, J. Phys IV France 104, 535-541 (2003)
6. Waddell, E.M., and Chapman, J.N., Optik 54, 2:82-96 (1979)
7. Polack, F., Joyeux, D., Phalippou, D., in *X-ray Microscopy and Spectromicroscopy*, Edited by J. Thieme et al, Springer, Berlin, 1998, pp. I-105-109
8. Feser, M., Jacobsen, C., Rehak, P. and DeGeronimo, G., J. Phys IV France 104, 529-534 (2003)
9. Morrison, G., *et al.,* J. Phys IV France 104, 547-550 (2003)
10. Maser, J., *et al.*, in *Design and Microfabrication of Novel X-Ray Optics*, Edited by D. Mancini, Ed., Proc. SPIE 4783, 2002
11. Divan, R., Mancini, D., Moldovan, N., Lai, B., Assoufid, L., Leonard, Q., Cerrina, F., Proc. SPIE 4783, 2002
12. Feser, M. *et a.l*, in *X-ray Micro- and Nano-focusing*, Edited by I. McNulty, Proc. SPIE 4499, 2001, pp 117-125
13. Feser, M., *Scanning Transmission x-ray Microscopy with a Segmented Detector*, Ph.D. Thesis, Stony Brook University, 2002